DOI 10.1007/s11041-021-00645-1
Metal Science and Heat Treatment, Vol. 63, Nos. 1 – 2, May, 2021 (Russian Original Nos. 1 – 2, January – February, 2021)

UDC 669.715:620.621.785.78

EFFECT OF PRELIMINARY TENSION AND CONDITIONS OF ARTIFICIAL AGING ON THE MICROSTRUCTURE AND PROPERTIES OF Al – Li ALLOY 2A97-T3

Peng Zhang[1] and Ming-He Chen[1]

Translated from *Metallovedenie i Termicheskaya Obrabotka Metallov*, No. 1, pp. 47 – 52, January, 2021.

The effect of various aging modes and preliminary tension (3%) on the microstructure and mechanical properties of Al – Li alloy 2A97-T3 (1.31% Li, 3.55% Cu, 0.37% Mg, the remainder aluminum) is studied. Scanning electron microscopy in combination with energy-dispersive spectroscopy and EBSD analysis are applied. The ultimate tensile strength is determined.

Key words: Al – Li alloys, artificial aging, preliminary tension, microstructure, texture.

INTRODUCTION

Alloys of the Al – Li system are very light structural materials used in aircraft and aerospace engineering [1 – 4] due to their low density, high strength and wear resistance, resistance to damage and stress corrosion cracking and to fatigue cracks [5, 6]. It is also expected that Al – Li alloys will replace the traditional high-strength aluminum alloys of series 2000 and 7000 [6 – 8]. Since the second-generation Al – Li alloys like 2090, 2091, 8090 and 8091 exhibit anisotropy, specialists work at Al – Li alloys of the third generation having a high resistance to impact loads [9, 10].

Precipitation-hardening alloy 2A97 of the third generation has been developed in China on the basis of the Al – Cu – Li system [6]. This high-alloy metal has a high ultimate strength and corrosion resistance, good weldability and resistance to impact loads, which explains its wide application. This is a promising material for the aerospace structural components including aircraft fuselage frame beams, stringers (high-strength beams and metallic structures passing through the whole of the body of the plane rendering it steady and strong), wing lower wall panels, and fuel storage tanks [11]. The properties of alloy 2A97 have been studied in a number of works. The authors of [6] have investigated the formation of microstructure and the mechanisms of superplastic deformation in a rolled alloy 2A97 at 390°C and the initial deformation rate of 3×10^{-3} sec^{-1}. The tensile strength and the elastic aftereffect in alloy 2A97 during the aging process and the contribution of various factors into these parameters have been studied in [12]. Fatigue tests of alloy 2A97 at room temperature have been performed in [11]. Formation of fatigue cracks and the phase precipitated at the early aging stages have been studied. In [13], tensile tests of alloy 2A97 have been conducted after a 3% and 6% preliminary deformation. The authors show that the preliminary deformation raises the ultimate tensile strength and lowers the elongation. The structure of the alloy is shown to contain precipitates of phases S' and T1 under the action of the preliminary deformation. The strength of the alloy and the phase precipitated under triple aging in the mode of retrogression and re-aging have been studied in [14]. The peak strength has been detected after the aging at 165°C under the T6 treatment. Works [15 – 19] have been devoted to the special features of friction stir welding and laser welding of the Al – Li alloy 2A97. A detailed study of the effect of the temperature and duration of solution treatment and of the aging modes on the microstructure and mechanical properties of 2A97 is described in [20]. The optimum temperature of the solution treatment is shown to be equal to 520°C at a 90-min hold. If the temperature of the first aging stage is high, and that of the second aging stage is low, the optimum combination of strength and ductility is obtained in the alloy after a short-term aging. Works [21, 22] are devoted to the relation between the corrosion behavior of alloy 2A97 and its structure and the precipitated phase. Despite the great number of studies of alloy 2A97, little attention has been devoted to the

[1] College of Mechanical and Electrical Engineering, Nanjing University of Aeronautics and Astronautics, Nanjing, China.

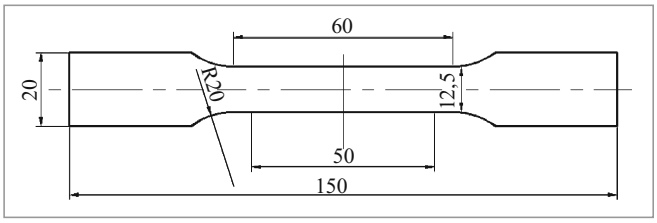

Fig. 1. A sample for tensile testing.

special features of its deformation and to formation of properties in different stages of the actual production process.

The properties of alloy AA97 after hot deformation with simultaneous quenching and artificial aging have been studied in [23 – 25] and those after the deformation in quenched condition have been studied in [26 – 28]. The results obtained may be used in an actual production of parts from this alloy in order to raise the operating capacity.

The aim of the present work was to perform a comparative analysis of the properties and microstructures of the Al – Li alloy 2A97 after deformation followed by different variants of aging and after aging without preliminary deformation.

METHODS OF STUDY

We studied a sheet from alloy 2A97 with a thickness of 1.5 mm produced by the Xi'an Aircraft Industry (Group) Co., Ltd. The alloy had the following rated chemical composition (in wt.%): 3.55 Cu, 1.31 Li, 0.37 Mg, 0.50 Zn, 0.31 Mn, 0.11 Zr, 0.044 Fe, 0.024 Ti, < 0.03 Ag, < 0.03 Si, 0.001 Be, the remainder Al.

The samples for the tensile tests were shaped a dog bone according to the GB/T228.1–2010 Standard. The sizes of the samples are given in Fig. 1. The samples were cut with the help of a wire electric discharge mill. The direction of the tension coincided with that of the rolling. The tensile tests were performed at room temperature at a constant strain rate of 0.01 sec^{-1} using a WDW-20E machine.

The sheet material was solution treated at 520°C for 90 min and then quenched in water at room temperature. A part of the samples was subjected to a preliminary 3% tension before the heat treatment. Then, the preliminarily deformed and not deformed samples were subjected to artificial aging.

To assess the deformability of the material we chose three modes of artificial aging basing ourselves on the earlier obtained results for alloy 2A97 [20], i.e., (*1*) 165°C, 60 h; (*2*) 200°C, 15 min + 165°C, 24 h; and (*3*) 200°C, 6 h + 165°C, 6 h with or without preliminary tension. After the aging, the samples were subjected to tensile tests at room temperature. The specimens for the EBSD study were cut using a wire electric spark mill from the region close to the fracture surface. The surface in the rolling plane was ground against a 1000 and 2000 sandpaper until disappearance of the surface scratches. Electropolishing was conducted in a 10% solution of perchloric acid in ethanol. The polishing electrolyte was cooled with liquid nitrogen. The electropolishing was conducted for 15 sec at a voltage of 20 V and a current of 0.9 – 1.0 A. A ZEISS ULTRA 55 field-emission scanning electron microscope was used for the EBSD and electron microscopy. The fracture surfaces were studied using a JSM-6360 scanning electron microscope in combination with a Genesis 2000XM60S energy dispersive spectrometer.

RESULTS AND DISCUSSION

To take into account the fine grains, the step for the EBSD analysis was chosen to be 4 μm. The data of the EBSD were processed using the fifth channel of the software for determining the gain boundary misorientation angle and the IPF diagram of the original sheet (Fig. 2). The grain boundaries with a misorientation angle below 10° were assumed to be small-angle ones and colored green. The boun-

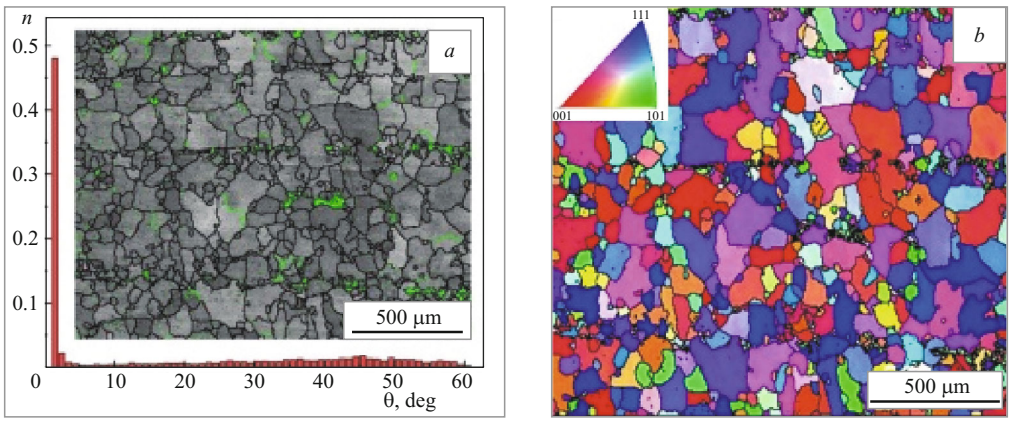

Fig. 2. Distribution of grains with respect to the misorientation angles θ (*n* is the relative frequency of the cases) (*a*) and inverse function of the distribution of grain orientations (*b*) in the original sheet of the Al – Li alloy.

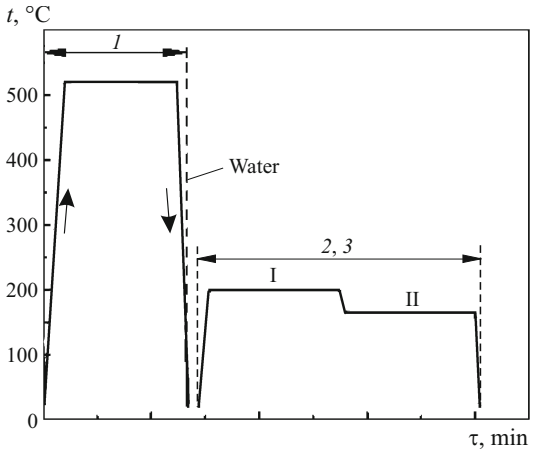

Fig. 3. Heat treatments of the Al – Li alloy: *1*) solution treatment (520°C, 90 min, water quenching); *2* and *3*) two-stage artificial aging with air cooling [(I) 200°C, 15 min + 165°C, 24 h and (II) 200°C, 6 h + 165°C, 6 h].

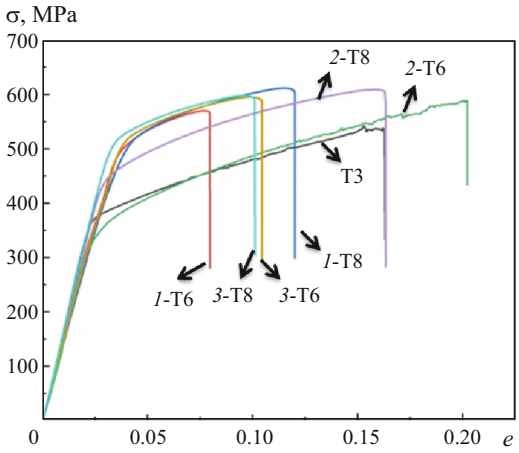

Fig. 4. True stress-strain curves of the Al – Li alloy 2A07 in different conditions: T6) after solution treatment and artificial aging; T8) after solution treatment, 3% tension, and artificial aging in modes *1*, *2*, and *3* [*1*) 165°C, 60 h; *2*) 200°C, 15 min + 165°C, 24 h; *3*) 200°C, 6 h + 165°C, 6 h].

daries with misorientation angle exceeding 10° were treated as large-angle ones and colored black. It can be seen from Fig. 2 that there are only few small-angle boundaries, while the large-angle boundaries are dominant. The heat treatment modes used for the alloy are presented in Fig. 3. After the heat treatment, the samples were subjected to tensile testing at room temperature. The results of the tests are presented in Fig. 4. It can be seen that the ultimate tensile strength and the yield strength increase substantially after the artificial aging and 3% preliminary tension. With allowance for the improvement of the properties and for the cost of the treatment, the best aging mode is 200°C, 6 h + 165°C, 6 h.

We studied the structure of the alloy after such aging with and without preliminary 3% tension. It can be seen from Fig. 5 that the number of small-angle boundaries near the fracture surface grows substantially, especially in the case of preliminary tension.

The tension conducted prior to artificial aging causes formation of dislocations in the matrix, which promotes uniform nucleation of particles of a δ′-phase (Al_3Li). Preliminary tension can also change the type and the distribution of the particles precipitated during aging. This will improve the mechanical properties and change the microstructure and the texture. The cooling after the homogenizing of the ingot from the Al – Li alloy produces rather coarse particles of phases T2 (Al_6Li_3Cu) and *R* (Al_5Li_3Cu) (Fig. 6*a* and *b*). In the case of preliminary 3% tension and aging at 200°C, 6 h + 165°C, 6 h, a lot of fine hardening particles of δ′-phase (Al_3Li) formed in the aging process are observable near the fracture surface (Fig. 6*c*). These particles are two orders of magnitude smaller than the particles in Fig. 6*a*. It seems that the particles observed in Fig. 6*c* are composite $Al_3(Li, Zr)$ formations due to precipitation of phase Al_3Li on the parti-

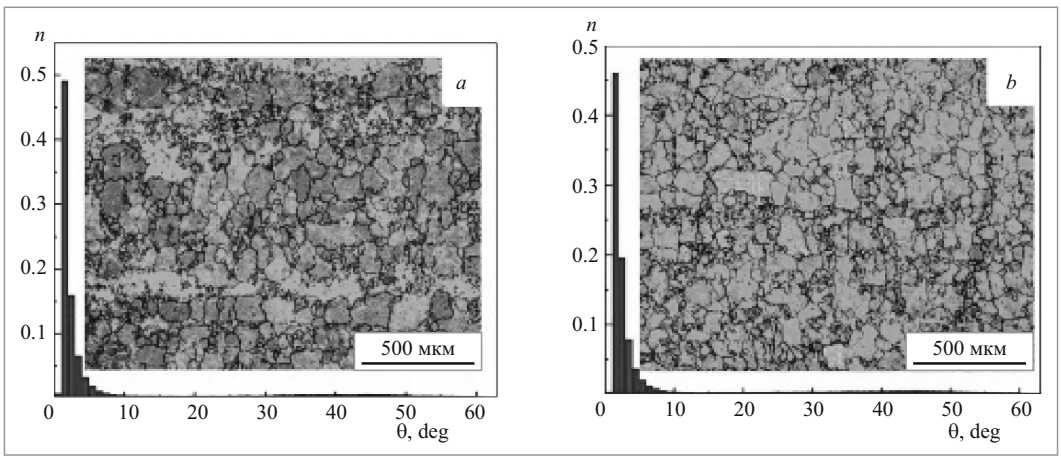

Fig. 5. Distribution of grains with respect to the misorientation angles θ (*n* is the relative frequency of the cases) for samples of the Al – Li alloy: *a*) without tension before the aging; *b*) with preliminary 3% tension.

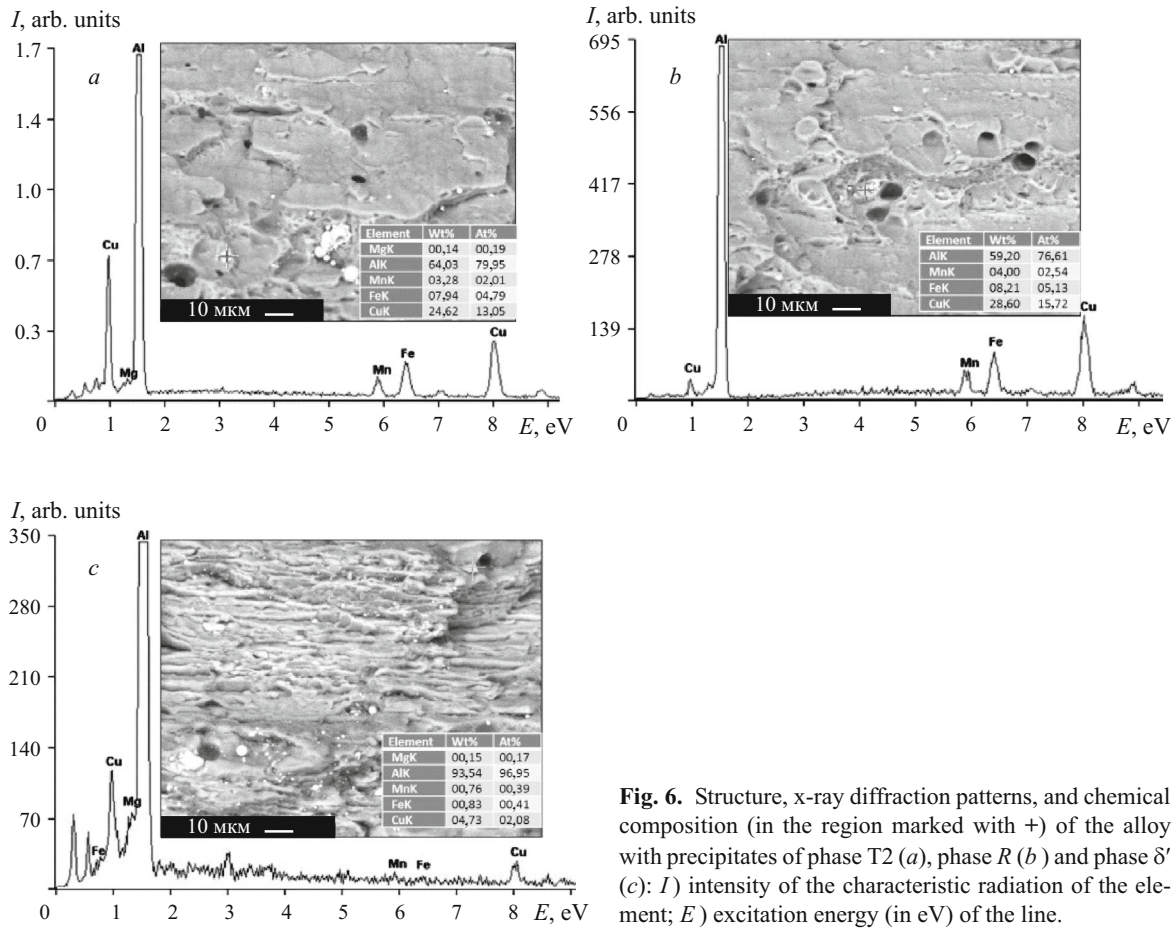

Fig. 6. Structure, x-ray diffraction patterns, and chemical composition (in the region marked with +) of the alloy with precipitates of phase T2 (*a*), phase *R* (*b*) and phase δ′ (*c*): *I*) intensity of the characteristic radiation of the element; *E*) excitation energy (in eV) of the line.

cles of Al_3Zr. This process may improve the mechanical properties of alloy 2A97.

To analyze the texture of the material in different conditions, we used the EBSD data to plot the functions of the distribution of grain orientations (Fig. 7), which allow us to make the following inferences.

1. The texture maximums of the material in the initial condition (Fig. 7*a*) correspond to Euler angles (4°, 38°, 45°); the orientation is describable as {112} $[1\bar{1}0]$, and the relative density of a maximum $f(g) = 11.1$.

2. The {112} $[1\bar{1}0]$ texture of the initial condition is weakened by the heat treatment and the artificial aging (Fig. 7*b*). The relative density of the orientation $f(g) = 7.56$.

3. The orientation of the strongest texture (53°, 88°, 45°) is describable as {110} [1 – 12] and $f(g) = 4.65$ (Fig. 7*c*), which is weaker than the texture presented in Fig. 7*b*.

4. After the tensile tests, an *S*-texture appears in Fig. 7*d* ; the strongest texture corresponds to angles (2°, 14°, 45°); the orientation is {116} [1 – 10] and its relative density $f(g) = 4.08$.

Artificial aging at 200°C, 6 h + 165°C, 6 h with preliminary deformation changes the texture as described above. The heat treatment causes precipitation of a hardening δ′-phase, and the mechanical properties of alloy 2A97 are improved substantially.

CONCLUSIONS

1. The ultimate strength and the yield strength of the Al – Li alloy 2A97-T3 increase after all the aging modes studied.

2. The best mode of artificial aging from the standpoint of the operating capacity of alloy 2A93-T3 and its production efficiency is a two-stage treatment 200°C, 6 h + 165°C, 6 h, which provides a yield strength of about 500 MPa at an elongation of about 10%.

3. In the initial condition, the structure of the alloy contains coarse particles of phases T2 and *R*; the fine δ′-phase precipitated under the aging preceded by 3% tensile deformation hardens the material.

4. Artificial aging with preliminary deformation changes the parameters of the crystallographic texture and lowers the density of the initial texture components.

The authors acknowledge the financial support of the National Natural Science Funds of China (Grant No. 51175252) and the technical support of the Ceshigo Research Service "www.ceshigo.com" in the EBSD study.

REFERENCES

1. Raj, Jenix Rino, John Xavier, Shanmugavel, Balasivanandha Prabu, "Thermal stability of ultrafine grained AA8090 Al – Li

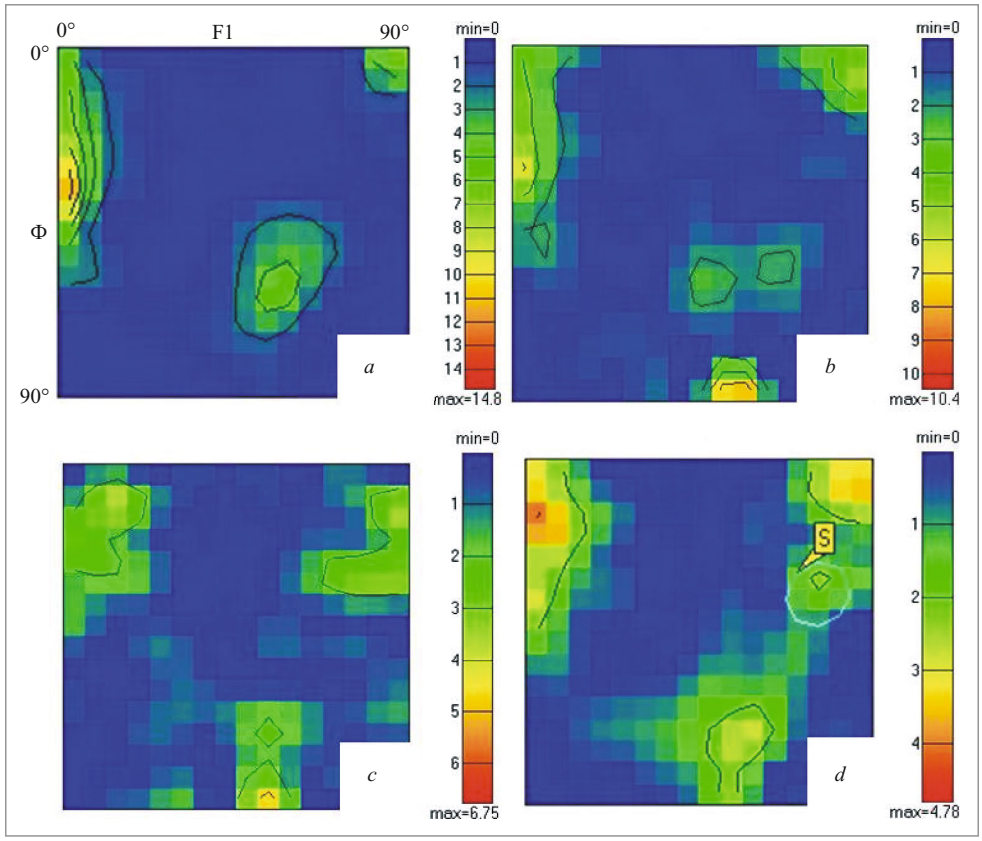

Fig. 7. Texture and the function of the distribution of the orientations (FDO) of grains at $\psi_2 = 45°$ for the Al – Li alloy in different states: *a*) initial; *b*) T6; *c*) T6 + tensile test; *d*) T8 + tensile test.

alloy processed by repetitive corrugation and straightening," *J. Mater. Res. Technol*., **8**(3), 3251 – 3260 (2019).
2. Liu, Fei, Zhiyi, et al., "Analysis of empirical relation between microstructure, texture evolution and fatigue properties of an Al – Cu – Li alloy during different pre-deformation processes," *Mater. Sci. Eng. A (Struct. Mater.: Prop., Microstr. Processing)*, **726**, 309 – 319 (2018).
3. Z. Jin, L. Zhide, X. Fushun, et al., "Regulating effect of pre-stretching degree on the creep aging process of Al – Cu – Li alloy," *Mater. Sci. Eng. A*, **763**(138157), 1 – 8 (2019).
4. Libin, Hu, Lihua, et al., "The effects of pre-deformation on the creep aging behavior and mechanical properties of Al – Li – S4 alloys," *Mater. Sci. Eng. A*, **703**, 496 – 502 (2017).
5. Y. Lin, C. Lu, C. Wei, et al., "Effect of aging treatment on microstructures, tensile properties and intergranular corrosion behavior of Al – Cu – Li alloy," *Mater. Character.*, **141**, 163 – 168 (2018).
6. L. Jia, R. Xueping, H. Hongliang, and Z. Yanling, "Microstructural evolution and superplastic deformation mechanisms of as-rolled 2A97 alloy at low-temperature," *Mater. Sci. Eng. A*, **759**, 19 – 29 (2019).
7. Z. Liwei, G. Wenli, G. Zhaohui, et al., "Hot deformation characterization of as-homogenized Al – Cu – Li X2A66 alloy through processing maps and microstructural evolution," *J. Mater. Sci. Technol*., **35**, 2409 – 2421 (2019).
8. A. Abd El-Aty, Y. Xu, X. Guo, et al., "Strengthening mechanisms, deformation behavior, and anisotropic mechanical properties of Al – Li alloys: A review," *J. Adv. Res*., **10**, 49 – 67 (2018).
9. T. Dursun and C. Soutis, "Recent developments in advanced aircraft aluminium alloys," *Mater. Design*, **56**, 862 – 871 (2014).
10. W. Fan, B. P. Kashyap, and M. Chaturvedi, "Anisotropy in flow and microstructural evolution during superplastic deformation of a layered-microstructured AA8090 Al – Li alloy," *Mater. Sci. Eng. A (Struct. Mater.: Prop., Microstr. Processing)*, **349**(1 – 2), 166 – 182 (2003).
11. J. Zhong, S. Zhong, Z. Q. Zheng, et al., "Fatigue crack initiation and early propagation behavior of 2A97 Al – Li alloy," *Trans. Nonferr. Met. Soc. China*, **24**(2), 303 – 309 (2014).
12. H. Y. Li and X. C. Lu, "Springback and tensile strength of 2A97 aluminum alloy during age forming," *Trans. Nonferr. Met. Soc. China*, **25**(4), 1043 – 1049 (2015).
13. C. Gao, Y. Luan, J. C. Yu, et al., "Effect of thermo-mechanical treatment process on microstructure and mechanical properties of 2A97 Al – Li alloy," *Trans. Nonferr. Met. Soc. China*, **24**, 2196 – 2202 (2014).
14. Z. S. Yuan, L. U. Zheng, Y. H. Xie, et al., "Effects of RRA treatments on microstructures and properties of a new high-strength aluminum-lithium alloy-2A97," *Chinese J. Aeronaut*., **20**, 187 – 192 (2007).
15. C. Gao, R, Gao, and Y. Ma, "Microstructure and mechanical properties of friction spot welding aluminium-lithium 2A97 alloy," *Mater. Design*, **83**, 719 – 727 (2015).
16. J. Ning, L. J. Zhang, Q. L. Bai, et al., "Comparison of the microstructure and mechanical performance of 2A97 Al – Li alloy joints between autogenous and non-autogenous laser welding," *Mater. Design*, **120** (Complete), 144 – 156 (2017).

17. H. Chen, L. Fu, P Liang, et al., "Defect features, texture and mechanical properties of friction stir welded lap joints of 2A97 Al – Li alloy thin sheets," *Mater. Charact*., **125**, 160 – 173 (2017).
18. H. Chen, L. Fu, and P. Liang, "Microstructure, texture and mechanical properties of friction stir welded butt joints of 2A97 AlLi alloy ultra-thin sheets," *J. Alloys Compd*., **92**, 155 – 169 (2017).
19. L. Chen, Y. N. Hu, E. G. He, et al., "Microstructural and failure mechanism of laser welded 2A97 Al – Li alloys via synchrotron 3D tomography," *Int. J. Lightweight Mater. Manuf*., **1**, 169 – 178 (2018).
20. H. Yan, *Study on the Heat Treatment Process and Microstructure Properties of the 2A97 Aluminum-Lithium Alloy [D]* [in Chinese], Hunan University (2010).
21. X. Zhang, X. Zhou, T. Hashimoto, et al., "The influence of grain structure on the corrosion behavior of 2A97-T3 Al – Cu – Li alloy," *Corros. Sci*., **116**, 14 – 21 (2017).
22. X. Zhang, X. Zhou, T. Hashimoto, et al., "Corrosion behavior of 2A97-T6 Al – Cu – Li alloy: The influence of non-uniform precipitation," *Corros. Sci*., **132**, 1 – 8 (2018).
23. G. Chen, M. Chen, N. Wang, et al., "Hot forming process with synchronous cooling for AA2024 aluminum alloy and its application," *Int. J. Adv. Manuf. Technol*., **86**, 133 – 139 (2016).
24. X. Fan, Z. He, K. Zheng, et al., "Strengthening behavior of Al – Cu – Mg alloy sheet in hot forming – quenching integrated process with cold – hot dies," *Mater. Design*, **83**, 557 – 565 (2015).
25. X. Fan, Z. He, S. Yuan, et al., "Experimental investigation on hot forming – quenching – integrated process of 6A02 aluminum alloy sheet," *Mater. Sci. Eng. A*, **573**, 154 – 160 (2013).
26. H. Li, X. Guo, W. Wang, et al., "Forming performance of an as-quenched novel aluminum-lithium alloy," *Int. J. Adv. Manuf. Technol*., **78**, 659 – 666 (2015).
27. M. L. Wang, P. P. Jin, J. H. Wang, et al., "Hot deformation behavior of as-quenched 7005 aluminum alloy," *Trans. Nonfer. Met. Soc. China*, **24**(9), 2796 – 2804 (2014).
28. X. W. Yang, Z. H. Lai, J. Zhu, et al., "Hot compressive deformation behavior of the as-quenched A357 aluminum alloy," *Mater. Sci. Eng. B (Adv. Funct. Solid-State Mater.)*, **177**, 1721 – 1725 (2012).